# Recent strategies for improving the performances of rechargeable lithium batteries with sulfur- and oxygen-based conversion cathodes

**Yao Ren, Jun-sheng Fan, Yong-zhu Fu***

College of Chemistry, Zhengzhou University, Zhengzhou 450001, Henan, China.

***Correspondence to:** Prof. Yongzhu Fu, College of Chemistry, Zhengzhou University, 100 Science Avenue, Zhengzhou 450001, Henan, China. E-mail: yfu@zzu.edu.cn

## Abstract

The energy density of lithium-ion batteries based on intercalated electrode materials has reached its upper limit, which makes it challenging to meet the growing demand for high-energy storage systems. Electrode materials based on conversion reactions such as sulfur, organosulfides, and oxygen involving breakage and reformation of chemical bonds can provide higher specific capacity and energy density. In addition, they usually consist of abundant elements, making them renewable. Although they have the aforementioned benefits, they face numerous challenges for practical applications. For example, the cycled products of sulfur and molecular organosulfides could be soluble in a liquid electrolyte, resulting in the shuttle effect and significant capacity loss. The discharged product of oxygen is $Li_2O_2$, which could result in high charge overpotential and decomposition of the electrolyte. In this review, we present an overview of the current strategies for improving the performances of lithium-sulfur, lithium-organosulfide, and lithium-oxygen batteries. First, we summarize the efforts to overcome the issues facing sulfur and organosulfide cathodes, as well as the strategies to increase the capacity of organosulfides. Then, we introduce the latest research progress on catalysts in lithium-oxygen batteries. Finally, we summarize and provide outlooks for the conversion of electrode materials.

**Keywords:** Electrode material, conversion reaction, sulfur, organosulfide, oxygen, lithium battery

## INTRODUCTION

In recent years, the enormous use of fossil fuels has caused severe environmental issues, including global warming, acid rain, and severe weather, leading to the usage increase of renewable energies such as solar and wind. To overcome the intermittent issue of these energies, energy storage systems are needed, such as rechargeable batteries. In addition, transportation electrification has been widely deployed as a means of reducing the use of fossil fuels. Among the rechargeable battery family, lithium-ion (Li-ion) batteries have been widely used as they have the highest energy densities. Traditional Li-ion batteries rely mostly on ion intercalation electrode materials, such as $LiCoO_2$, $LiMn_2O_4$, and $LiFePO_4$, which have limited capacities and energy densities[1,2]. During repeated charge and discharge of the battery, Li ions are repeatedly intercalated and de-intercalated from the electrode material, resulting in structural changes in the active material and a decrease in capacity[3]. Moreover, Li-ion batteries rely mostly on transition metals, such as cobalt, nickel, manganese, *etc.*, and the transition metal resources are limited, which is contrary to the current concept of sustainable development[4]. As a result, an increasing number of researchers are working on the development of high-energy-density, environmentally friendly, and safe rechargeable batteries in an effort to change the status quo.

Different from ion intercalation electrode materials, conversion-based electrode materials rely on the breakage and formation of chemical bonds. For instance, the sulfur cathode relies on the reversible breakage and reformation of sulfur-sulfur (S-S) bonds, which leads to a high theoretical specific capacity (1,675 mAh $g^{-1}$) and energy density (2,600 Wh $kg^{-1}$)[5]. Although conversion-based electrode materials have many advantages and great competitiveness, there are still some problems preventing their practical applications. Take sulfur[6], organosulfide[7], and oxygen electrodes[8] as examples: organosulfides like sulfur are also based on the breakage and reformation of S-S bonds. Both sulfur and organosulfides have similar issues, such as low electronic conductivity and high solubility of intermediates, resulting in continuous loss of active materials and rapid capacity decay. The discharged product ($Li_2O_2$) of oxygen is insulating and difficult to decompose, resulting in a high overpotential of the oxygen evolution reaction (OER) during the charge and low electrochemical reversibility[9].

In this review, recent advances in sulfur, organosulfide, and oxygen as cathode materials are reviewed, as shown in Figure 1. In Section "SULFUR CATHODE", some strategies are listed, including host materials to improve conductivity, separator modification to reduce the shuttle effect, functional electrolyte additives to alter the redox path of sulfur, and electrode-electrolyte interface enhancement to improve stability. In the Section "ORGANOSULFIDE CATHODE", we summarize the use of transition metal compounds to alleviate the solubility problem of organosulfides and their discharge products, the development of organosulfide polymers to increase their theoretical specific capacities, and the application of solid-state electrolytes to improve battery safety and eliminate the undesirable shuttle effect. In the Section "OXYGEN CATHODE", the recent development of catalysts to facilitate the delithiation of $Li_2O_2$ and reduce the occurrence of side reactions during charging is presented. In summary, we provide an overview of the most recent developments in representative cathode materials based on conversion reactions. Finally, future developments and outlooks are given.

## SULFUR CATHODE

The sulfur cathode has advantages such as low cost, abundant resources, high theoretical capacity, and high energy density[10]. It has been widely studied in recent years and is considered as the most promising electrode material in next-generation energy storage systems. During discharge, the sulfur cathode goes through a "solid-liquid-solid" conversion process in which the solid sulfur element ($S_8$) is first converted into soluble lithium polysulfides $Li_2S_x$ ($3 \le x \le 8$) and then into solid $Li_2S_2/Li_2S$. The overall charge/discharge
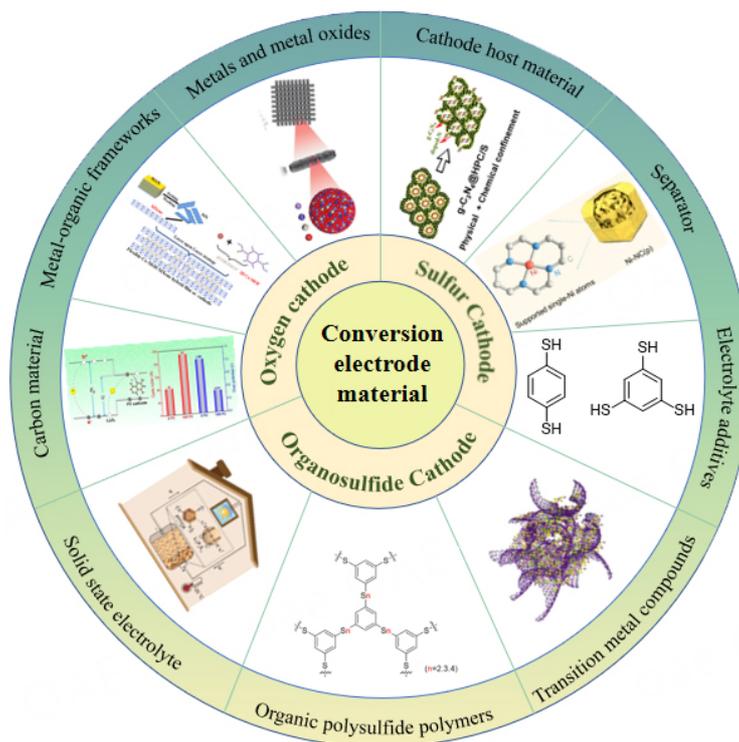
**Figure 1.** Summary illustration of the research progress of conversion electrode materials. Reproduced with permission from Ref.[11] (Copyright 2020, Elsevier), Ref.[12] (Copyright 2022, Wiley-VCH GmbH), Ref.[13] (Copyright 2021, American Chemical Society), Ref.[14] (Copyright 2021, Nature Publishing Group), Ref.[15] (Copyright 2019, Elsevier), Ref.[16] (Copyright 2021, Elsevier), Ref.[17] (Copyright 2021, Wiley-VCH GmbH), Ref.[18] (Copyright 2022, Elsevier), Ref.[19] (Copyright 2021, Elsevier), Ref.[20] (Copyright 2021, Wiley-VCH GmbH).

processes of $S_8$ can be described in Equation (1). In fact, the concept of the sulfur cathode was first proposed in the 1960s, but it was ignored due to its drawbacks, such as low discharge capacity and fast capacity decay. Studies of sulfur cathode were rare until 2009, when Ji *et al.* successfully cycled the Li-S battery for 20 cycles using CMK-3 as the sulfur host material[21]. Sulfur cathode suffers from three major issues: (1) sulfur and its cycled products are electronic and ionic insulators, resulting in low sulfur utilization and discharge capacity[22]; (2) the $Li_2S_x$ formed during cycling is easily soluble in the ether electrolyte and shuttle from the cathode to the anode during discharge, which results in low Coulombic efficiency and rapid capacity decay; and (3) due to the difference in density (S: 2.07 g cm$^{-3}$, Li$_2$S: 1.66 g cm$^{-3}$), Li$_2$S formed after full discharge causes serious volume expansion, resulting in poor battery cycle performance[23]. This section summarizes the works that were published during the last three years, including sulfur host materials, separator modifications, and electrolyte additives.

$$S_8 \xleftrightarrow{\quad Li_2S_x \, (3 \leq x \leq 8) \quad} Li_2S_2/Li_2S \tag{1}$$

**Sulfur host materials**

The most direct and fundamental strategy to address the current issues of the sulfur cathode is to develop various sulfur host materials. It can improve the practical application value of Li-S batteries and help to address the intrinsic drawbacks of non-conductive $S/Li_2S_x$ ($1 \leq x \leq 2$) and shuttle of lithium polysulfides (LiPSs). Conductive carbon materials, such as mesoporous carbon, hollow carbon nanosphere, carbon nanotubes (CNTs), and graphene, are now the most well-known Li-S cathode host materials[24]. They can

improve the conductivity of the cathode and physically contain LiPSs, thereby inhibiting the dissolution and shuttle of LiPSs. However, the actual demand is still far from being met by the improved performance of the mentioned host materials in Li-S batteries. As a result, numerous new host materials have been developed over time, including porous carbon with a large surface area and high porosity, carbon materials doped with polar elements like N and S, and the employment of metals and metal compounds. Table 1 lists the electrochemical properties of different sulfur host materials in Li-S batteries.

*Carbon-based host materials*

Hu *et al.* used a double alkali activation process to prepare coral-like graded porous carbon, which has a higher specific surface area (2,004 $m^2 g^{-1}$) and larger pore volume (1.64 $cm^3 g^{-1}$) than ordinary porous carbon[25]. The pore parameters can also be precisely adjusted by the pore creators. Large pores in hierarchical porous carbon can shorten the transport path of $Li^+$ and increase sulfur content. Mesopores can hold sulfur nanoparticles, and micropores can adsorb LiPSs to inhibit the dissolution and shuttling. As shown in Figure 2A, Zhang *et al.* activated porous carbon nanotube microspheres (ePCNTMs) by "Sauna", which is a scalable spray drying method for critical water vapor etching at high temperatures. It can construct rich topological defects in the carbon lattice. The ePCNTMs, as the host material, has strong adsorption and catalytic activity[26]. Due to the weak interaction between carbon materials and LiPSs, it is certain that some LiPSs would dissolve and shuttle; hence, efforts have been made to dope carbon materials with polar components. As depicted in Figure 2B, Shi *et al.* synthesized several carbon-based host materials (CR-PPIs@800) from crosslinked polyimides via a series of straightforward processes[27]. The porous network structure of CR-PPIs@800 allows high sulfur content and volume expansion upon cycling in batteries. It also contains a high concentration of polar N due to the electrophilicity of $Li^+$ and the electronegativity of N (3.04), which can lead to strong chemical adsorption on LiPSs, hence inhibiting the dissolution of LiPSs effectively. Similarly, Liu *et al.* produced N-doped hollow porous carbon spheres (N-HPCS) using biomass lignin as the precursor and cyanuric acid as the N-dopant and porogen [Figure 2C][28]. Sulfur can be encapsulated in hollow carbon spheres with high content. Using wheat as a raw material, Hong *et al.* fabricated a hundred-gram of a graphitic carbon nitride@hierarchical porous carbon (g-$C_3N_4$@HPC) composite [Figure 2D][11], in which HPC can physically contain LiPSs and restrict the volume expansion of S, while g-$C_3N_4$ can chemically adsorb LiPSs. Yang *et al.* used activated carbon (AC) with $Al_2O_3$@$SiO_2$ heterojunction as the S host material[29]. The AC has a large specific surface area (906.4611 $m^2 g^{-1}$) and is coupled with a portion of the S cathode material replaced by selenium (Se) and tellurium (Te). Small amounts of Se and Te are added to S to compensate for its poor conductivity. After 300 cycles, SST811/AC (where S/Se/Te = 8:1:1, molar ratio) still retains a capacity of 1,024.9 mAh $g^{-1}$.

*Metals and metal compounds*

The introduction of metals in carbon-based materials or the use of metal compounds is the typical way to improve the electrochemical performance of Li-S batteries. The non-polar carbon-based host materials interact with LiPSs via weak van der Waals force, while metals and metal compounds can chemically adsorb LiPSs by forming M-S (M: metal) bonds[30]. Compared with the weak van der Waals force, the M-S bonds are stronger, and the inhibition of the shuttle effect is more effective. Metals can also catalyze the conversion of high-order LiPSs to $Li_2S_2$/$Li_2S$, lower the energy barrier, and accelerate the kinetics of the reaction.

Li *et al.* utilized a $NH_4Cl$-assisted pyrolysis strategy to produce highly mesoporous N-rich carbon with a thin shell and porous internal network, which is fixed on the top side of single Ni atoms [designed as Ni-NC(p)] [Figure 3A] as the host material for Li-S batteries[12]. High mesopores facilitate electron/ion transport, increase sulfur content and utilization, and inhibit volume expansion. Through physicochemical adsorption, the N-rich shells can anchor LiPSs. At the same time, single Ni atoms can promote the

**Table 1. Electrochemical properties of different sulfur host materials in Li-S batteries**

| Sulfur host | Discharge capacity | Cycles | Ref. |
| --- | --- | --- | --- |
| coral-like hierarchical porous carbon | 1,112 mAh g$^{-1}$ at 0.1 C | 500 at 0.5 C | [25] |
| ePCNTM | 1,067 mAh g$^{-1}$ after 100 cycles at 0.2 C | 500 at 1 C | [26] |
| CR-PPIs@800 | 1,100 mAh g$^{-1}$ at 0.1 C | 1,100 at 1 C | [27] |
| N-HPCS | 1,535.1 mAh g$^{-1}$ at 0.1 C | 1,000 at 1 C | [28] |
| g-C$_3$N$_4$@HPC | 804.1 mAh g$^{-1}$ at 1 C | 250 at 1 C | [11] |
| AC with an Al$_2$O$_3$@SiO$_2$ heterojunction | 1,171.7 mAh g$^{-1}$ at 0.5 C | 300 at 1 C | [29] |
| Ni-NC(p) | 966.6 mAh g$^{-1}$ (3rd cycle) at 0.5 C | above 600 at 0.5 C | [12] |
| CR-Por-Cu-PPI@800 | 1,064 mAh g$^{-1}$ at 0.2 C | 500 at 1 C | [31] |
| Co@N-HCMSs | 1,172 mAh g$^{-1}$ at 0.2 C | 500 at 1 C | [32] |
| PCPC/NiCoP | 1,462.7 mAh g$^{-1}$ at 0.1 C (pouch cell) | above 60 at 1 C (pouch cell) | [33] |
| MoC/NC CSMSs | 1,370.3 mAh g$^{-1}$ at 0.1 C | 500 at 1 C | [34] |
| Co$_x$S$_y$/MnS/NC@NC | 890.7 mAh g$^{-1}$ at 0.1 C | 500 at 1 C | [35] |
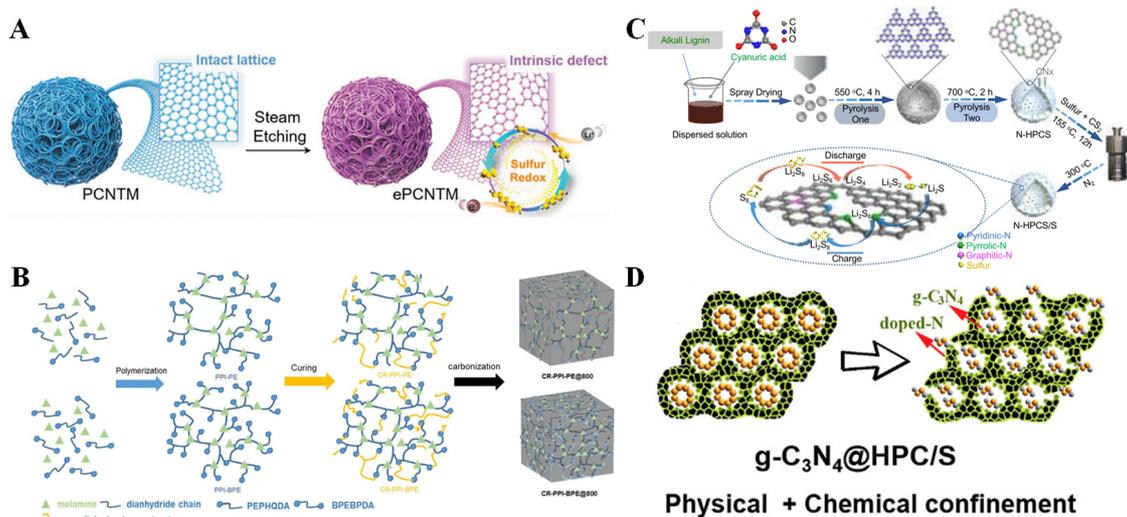


**Figure 2.** (A) Schematic diagram of "sauna" activation of ePCNTM. Reproduced with permission from Ref.[26] (Copyright 2021, Wiley-VCH GmbH). (B) Schematic illustration of CR-PPIs@800 synthesis. Reproduced with permission from Ref.[27] (Copyright 2022, Elsevier). (C) Schematic diagram of the synthetic route of N-HPCS/S and its interaction with polysulfides. Reproduced with permission from Ref.[28] (Copyright 2020, Wiley-VCH GmbH). (D) Dual physical/chemical confinement of LiPSs by g-C$_3$N$_4$@HPC. Reproduced with permission from Ref.[11] (Copyright 2020, Elsevier).

conversion of LiPSs, effectively inhibiting the shuttle effect. The results show that the sulfur cathode with Ni-NC(p) exhibits a high specific capacity, good rate performance, and cycle stability. Lin *et al.* fabricated several carbon-based metal-doped materials (CR-Por-PPIs@800) by crosslinking porous porphyrin-based polyimides and employed them as sulfur hosts[31]. Doping metals help reduce reaction activation energy and accelerate reaction kinetics. As shown in Figure 3B, the copper-doped one has the most stable cycle stability, with a capacity of 520 mAh g$^{-1}$ after 500 cycles. Su *et al.* synthesized cobalt (Co) embedded N-doped hollow carbon microspheres (Co@N-HCMSs) as the sulfur host material [Figure 3C][32]. Hollow carbon microspheres can contain sufficient sulfur and restrict its volume expansion while also physically storing LiPSs. Co nanoparticles coated on the pore wall can activate N-HCMSs, enhance their adsorption, and catalyze the conversion of LiPSs. Utilizing Co@N-HCMSs as the host material enables the Li-S battery to have a high area capacity of approximately 5 mAh cm$^{-2}$ at a high sulfur concentration (90.5 wt%).
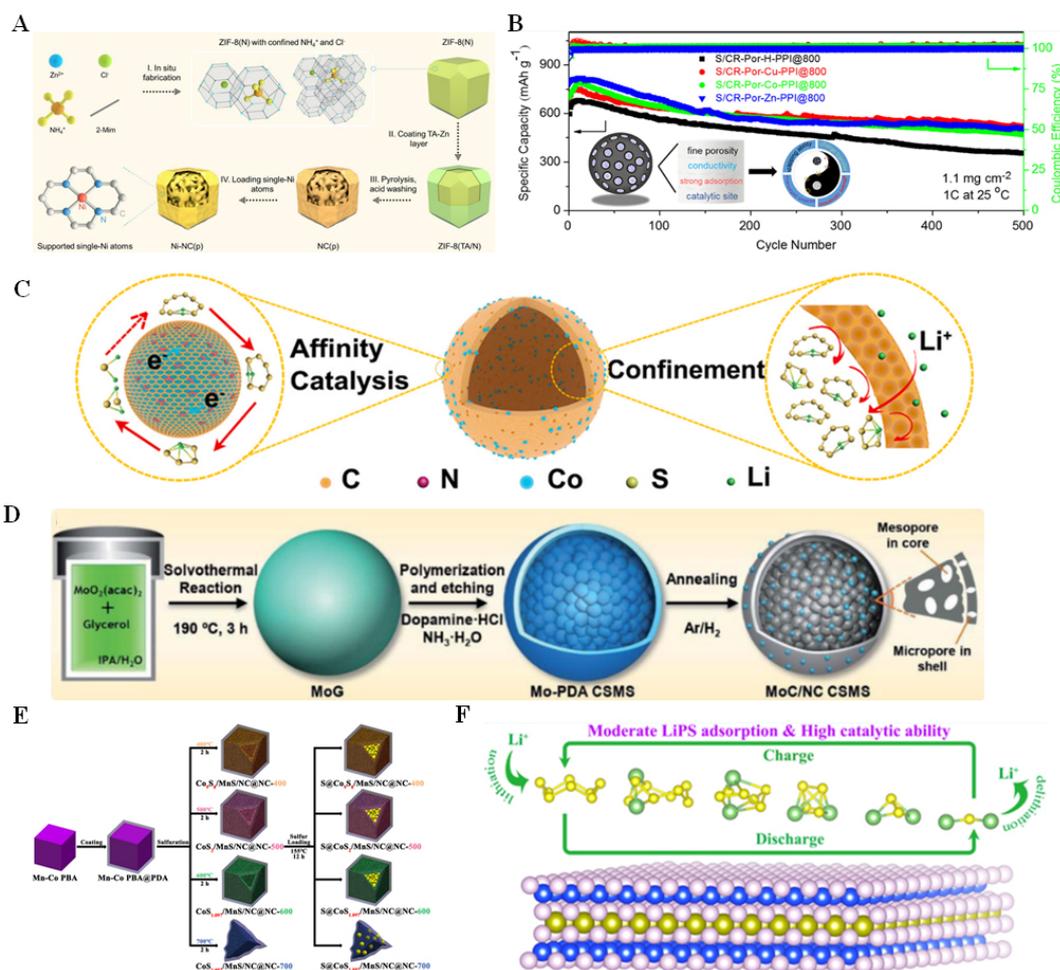
**Figure 3.** (A) Schematic diagram of Ni-NC(p) preparation route. Reproduced with permission from Ref.[12] (Copyright 2022, Wiley-VCH GmbH). (B) Cycle performance at 1 C with different host materials. Reproduced with permission from Ref.[31] (Copyright 2021, American Chemical Society). (C) Mechanism diagram of porous carbon microspheres with multiple effects on Li-S batteries. Reproduced with permission from Ref.[32] (Copyright 2021, Elsevier). (D) Schematic diagram of MoC/NC CSMS synthesis. Reproduced with permission from Ref.[34] (Copyright 2021, The Royal Society of Chemistry). (E) S@Co$_x$S$_y$/MnS/NC@NC synthesis process schematic. Reproduced with permission from Ref.[35] (Copyright 2022, Elsevier). (F) Schematic diagram of the interaction between two-dimensional MSi$_2$P$_4$ (M = V, Nb, and Ta) monolayers and LiPSs. Reproduced with permission from Ref.[36] (Copyright 2022, American Chemical Society).

Zhang *et al*. implanted NiCoP nanoparticles into petroleum coke (PCPC)-derived N, S co-doped porous carbon and utilized them as sulfur host materials[33]. PCPC with a large specific surface area can provide great adsorption sites, and N, S co-doping is conducive to enhancing the utilization of S, while the incorporation of NiCoP nanoparticles facilitates the conversion of LiPSs. As shown in Figure 3D, Li *et al*. prepared meso-/microporous core-shelled MoC nanocrystal-embedded N-doped carbon microspheres (MoC/NC CSMSs) as the host material for sulfur[34]. The shell of the MoC/NC CSMSs is microporous, while the pore core is mesoporous, assuring a high sulfur content. The evenly distributed MoC binds with LiPSs chemically, forming Mo-S bonds. The battery shows an initial discharge specific capacity of 1,370.3 mAh g$^{-1}$ at 0.1 C. Defective transition metal compound materials have strong binding energies with sulfur and can effectively inhibit the shuttle of LiPSs. As shown in Figure 3E, Kang *et al*. designed and synthesized four Co$_x$S$_y$/MnS/NC@NC materials with defective hollow nanocubes (NC: nitrogen-doped carbon) as the sulfur host materials[35], which could inhibit the volume expansion of sulfur, catalyze the conversion of LiPSs,

reduce the shuttle of LiPSs, and improve the reaction kinetics of batteries. Wang *et al.* employed the two-dimensional, monolayer $MSi_2P_4$ (M = V, Nb, and Ta) as the sulfur host material [Figure 3F][36]. The $MSi_2P_4$ monolayer can also absorb polysulfides, reduce the reaction barrier, and accelerate the conversion of LiPSs when $S_8/Li_2S_x$ are immobilized on its surface without structural deformation. This effectively improves the capacity retention and cycle stability of the battery.

## Separator

The separator is an important part of the battery. In order to improve the performance of sulfur cathodes, the functionalization of separators is a well-established technique for suppressing LiPSs shuttle and enhancing battery cycling performance. The separator affects the interface structure and internal resistance of the battery, which directly impacts the discharge capacity, cycle life, and safety[37]. The functionalized separator must have the following characteristics: (1) it should be a good insulator; (2) it has a certain pore size and porosity, ensuring low resistance and high ion conductivity; and (3) it should be resistant to electrolyte corrosion and has good electrolyte wettability. Over the past years, many efforts have been focused on the separator modification or interlayers between the separator and sulfur cathode to improve the electrochemical performance of Li-S batteries.

### *Separator modifications*

Wu *et al.* synthesized a N, S co-doped carbon framework (NSPCF) with contained $CoS_2$ nanoparticles and rooted carbon nanotubes (NSPCF@$CoS_2$), which was coated on a separator to improve the electrochemical performance of Li-S batteries, as shown in Figure 4A[38]. The CNT structure not only has a physical adsorption effect on LiPSs but also improves charge transfer, and $CoS_2$ captures LiPSs via Lewis acid-base interaction to enhance sulfur utilization. Wang *et al.* developed the LiX@Celgard (LiX: Li-ion exchanged X-type zeolite) separator [Figure 4B] using an *in situ* hydrothermal synthesis method. It improves electrolyte wettability and suppresses LiPSs shuttle[39]. Compared to the Celgard separator, the LiX@Celgard separator exhibits higher lithium-ion conductivity and diffusion coefficient. Wang *et al.* immobilized CoFe alloy *in situ* within a N-doped carbon nanocube (CoFe@NC) in order to achieve the catalytic conversion of LiPSs [Figure 4C][40]. CoFe@NC serves a dual function. It can not only chemically adsorb and impede shuttles of LiPSs, but also catalyze the conversion of LiPSs and enhance the battery reaction kinetics. Yu *et al.* proposed a method to suppress the shuttle of the LiPSs by reducing the pore size of the separator[41]. Since the pores of the separator are microsized, a polymer with intrinsic nanoporosity (PIN) is designed within the pores. The separator is employed as a skeleton to preserve the good mechanical properties of its own, and the thickness of the separator is maintained. The PIN allows the transport of $Li^+$ but suppresses LiPSs shuttle. Peng *et al.* proposed the use of $NiFe_2O_4$ quantum dots (QDs) and $g-C_3N_4$ nanofibers to improve the heat resistance of the separator[42]. The $NiFe_2O_4$ QDs@$g-C_3N_4$ modified separator has superior flexibility and mechanical strength. It also allows rapid movement of lithium ions and enhances energy storage efficiency. In addition, the inherent non-flammability and high melting point of $NiFe_2O_4$ and $g-C_3N_4$ nanofibers help reduce the risk of combustion and the explosion of Li-S batteries [Figure 4D].

### *Interlayers*

Tan *et al.* explored a thin and light (8 μm and 0.24 mg cm$^{-2}$) interlayer consisting of reduced graphene oxide@$MoS_2$ (rGO@$MoS_2$) [Figure 5A][43]. rGO is mainly responsible for physical adsorption and conductivity, whereas $MoS_2$ is primarily responsible for the chemical adsorption of LiPSs. The Li-S battery with the interlayer shows a high reversible capacity of 1,122 mAh g$^{-1}$ at 0.2 C. Hu *et al.* embedded $CoS_2$ in hierarchical porous graphitic carbon (HPGC) as an interlayer, as shown in Figure 5B[44]. It has a high specific surface area that can be used to adsorb LiPSs, and high conductivity facilitates charge transfer. The Li-S battery with the interlayer can be stably cycled for 500 cycles at 1 C. Kim *et al.* designed a hierarchical $Fe_3O_4/C_3N_4$ nanostructure as a multifunctional interlayer[45]. $C_3N_4$ nanotubes have a high affinity for LiPSs
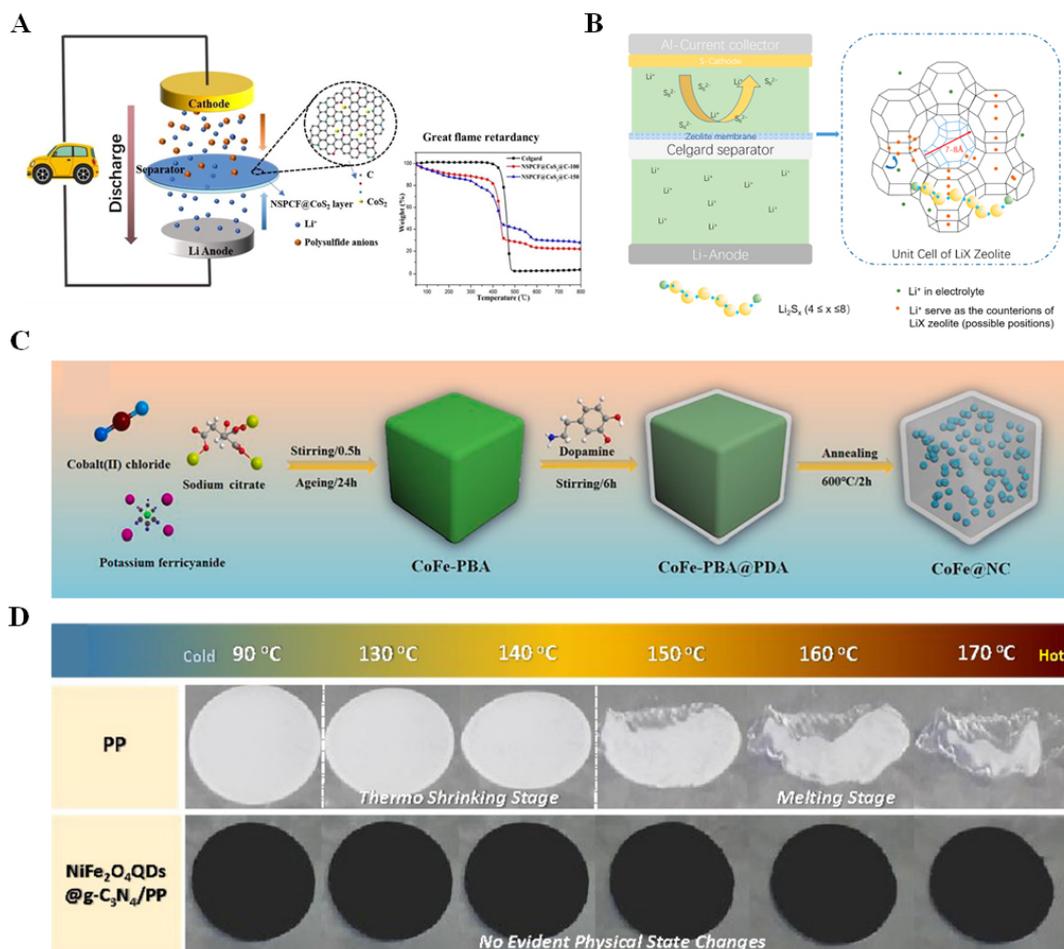
**Figure 4.** (A) Working mechanism of modified separator in Li-S battery. Reproduced with permission from Ref.[38] (Copyright 2021, Elsevier). (B) LiX zeolite membrane-coated Celgard is used as the design principle of the separator. Reproduced with permission from Ref.[39] (Copyright 2020, Elsevier). (C) Schematic diagram of the synthesis of the CoFe@NC. Reproduced with permission from Ref.[40] (Copyright 2021, Elsevier). (D) Comparison of thermal stability of pp and NiFe$_2$O$_4$ QDs@g-C$_3$N$_4$/PP. Reproduced with permission from Ref.[42] (Copyright 2022, The Royal Society of Chemistry).

and a large surface area. The surface-modified Fe$_3$O$_4$ nanospheres accelerate polysulfide adsorption and enhance electron transport. As depicted in Figure 5C, when a battery undergoes 1,000 cycles at 2 C, the capacity loss rate per cycle is as low as 0.02%. As shown in Figure 5D, Lee *et al.* designed and made a redox-active interlayer consisting of a sulfur-impregnated composite of polar platelet ordered mesoporous silica (abbreviated as pOMS/S$_x$, where *x*% is the weight ratio of sulfur in the composite)[46]. First of all, pOMS/S$_x$ can add more active sulfur and increase the area capacity without adding more inactive material. Moreover, polar pOMS/S$_x$ interlayer may effectively anchor dissolved LiPSs on the surface or in the porous structure via polar-polar interactions. Thereby, it prevents the shuttle effect of LiPS corrosion of lithium metal and enhances the cycle stability of the battery.

### Electrolyte additives

The ether electrolyte used in Li-S battery is typically composed of 1.0 M lithium bis(trifluoromethanesulfonyl) imide (LiTFSI) and 1.0 wt% lithium nitrate (LiNO$_3$) in a mixture solvent of 1,2-dimethoxyethane (DME)/1,3-dioxolane (DOL) (1:1 *v/v*). Electrolyte additives can have significant effects on the following aspects of Li-S batteries, such as altering the redox path of S, enhancing the stability
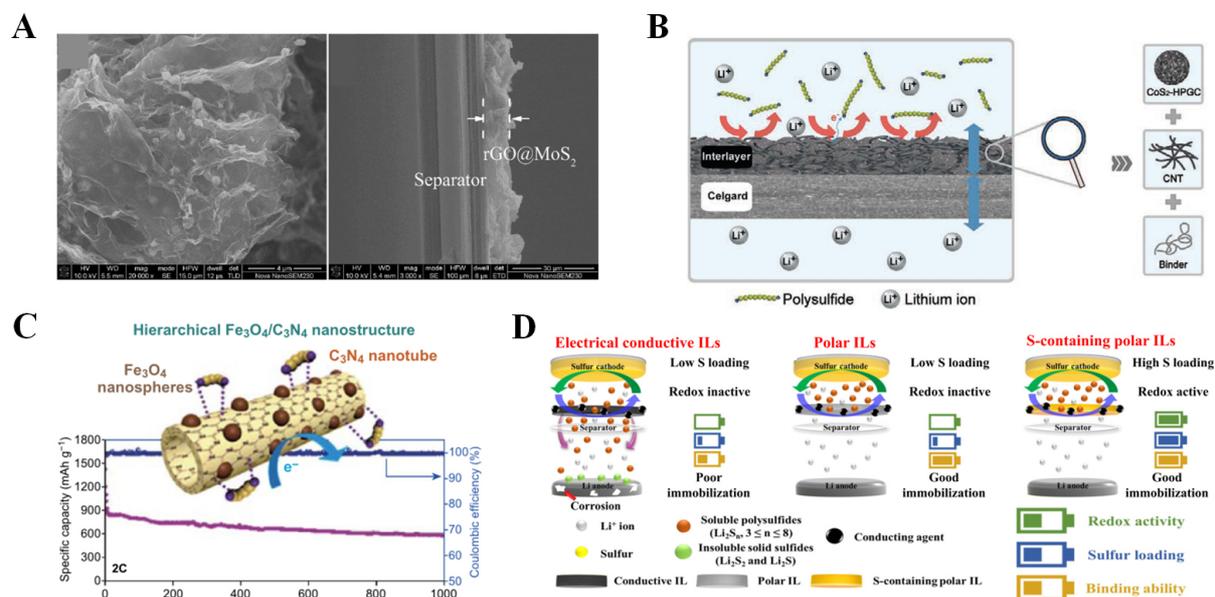
**Figure 5.** (A) Scanning electron microscope (SEM) image of rGO@MoS$_2$ composite on the separator. Reproduced with permission from Ref.[43] (Copyright 2018, American Chemical Society). (B) Schematic diagram of the interaction between CoS$_2$/HPGC interlayer and LiPSs. Reproduced with permission from Ref.[44] (Copyright 2022, Wiley-VCH GmbH). (C) Hierarchical Fe$_3$O$_4$/C$_3$N$_4$ nanostructure diagram and cycle performance at 2 C rate. Reproduced with permission from Ref.[45] (Copyright 2020, Springer). (D) Design principles for redox-active interlayer. Reproduced with permission from Ref.[46] (Copyright 2022, Nature Publishing Group).

of the electrode/electrolyte interface, and inhibiting the growth of lithium dendrites. In addition, the development of functional additives is an economical and efficient approach to improving the electrochemical stability of Li-S batteries[47].

As shown in Figure 6A, Guo *et al.* introduced a bifunctional electrolyte additive to Li-S electrolyte, i.e., 1,3,5-benzenetrithiol (BTT)[14]. BTT can react with lithium metal to build a layer of organic-inorganic composite SEI on the anode, inhibiting the growth of lithium dendrite. At the same time, BTT also reacts with sulfur to generate oligomer/polymer organosulfur, thereby effectively reducing the loss of active material and improving the utilization of S. Lian *et al.* selected three benzenedithiols as electrolyte additives and experimentally proved that 1,4-benzenedithiol (1,4-BDT) among the three isomers has the best electrochemical performance[13]. On the one hand, 1,4-BDT forms an effective SEI at the lithium metal surface and improves the interface stability of the anode. On the other hand, it can react with S to generate S-S bonds, change the redox path of S, and inhibit the lithium polysulfide shuttle [Figure 6B]. Similar to thiophenol, benzoselenol (PhSeH) can also be used as an electrolyte additive for Li-S batteries, and the mechanism is similar. Sun *et al.* added PhSeH to the electrolyte[48], and the electrochemical performance was significantly improved. The discharge capacity is as high as 1,436 mAh g$^{-1}$ after 200 cycles, and there is still a capacity retention rate of 92.86%. In addition, the battery overpotential is significantly reduced. As shown in Figure 6C, the pouch cell with a low E/S ratio of 4.0 μL mg$^{-1}$ can also be stably cycled for 20 cycles. Wang *et al.* introduced triazole (Ta) and tetrazole (Tta) into the electrolyte[49]. First of all, there are lithium bonds between azole compounds and LiPSs, which can assist in the redox process. Secondly, it also interacts with lithium salts in the electrolyte, increasing ionic conductivity and lithium-ion transference number. Finally, it can promote the uniform deposition of lithium and improve battery safety. Jiang *et al.* applied 1,3,5-triformylphloroglucinol (TFP) as an electrolyte additive[50]. TFP can react with LiPSs *in situ* to generate insoluble organic polysulfides, improving oxidation reaction kinetics. The newly generated organic polysulfides exist in the form of aggregated nanoparticles, which can adsorb unreacted polysulfides.
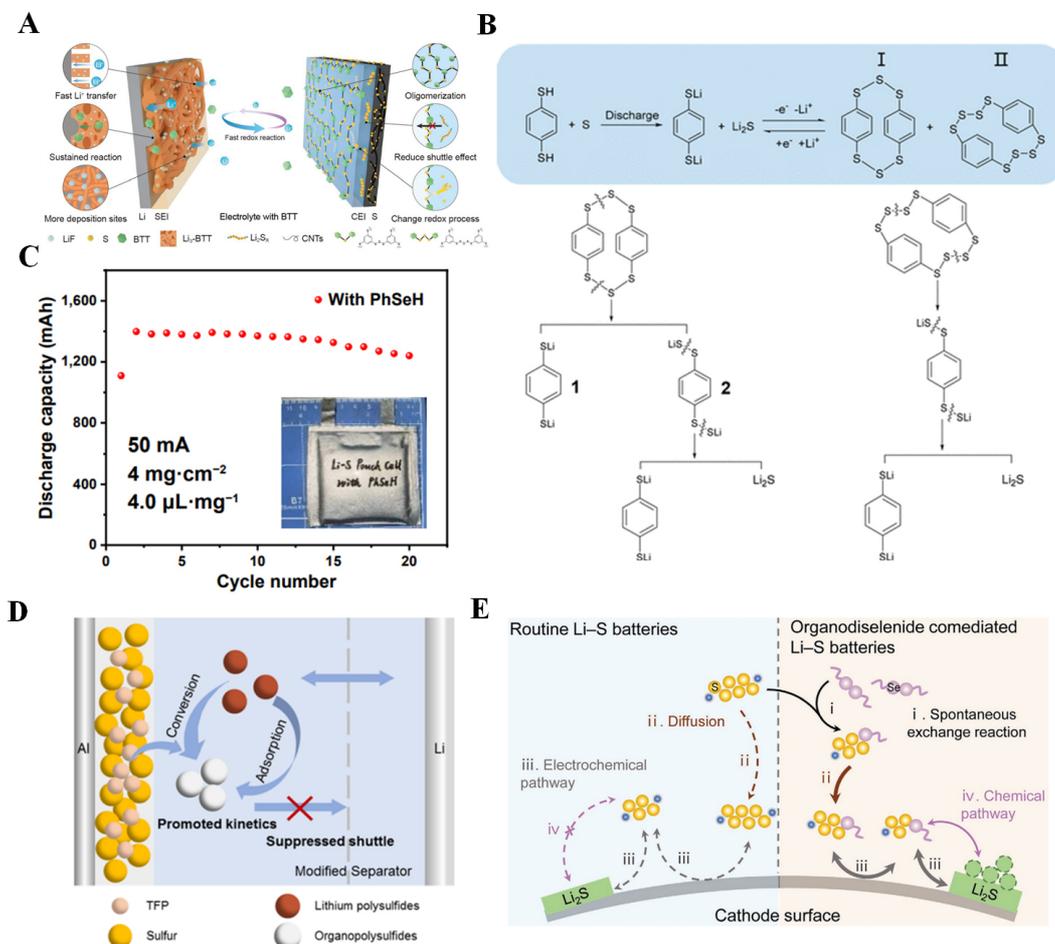
**Figure 6.** (A) Schematic diagram of a Li-S battery with BTT. Reproduced with permission from Ref.[14] (Copyright 2021, Nature Publishing Group). (B) Possible reduction reactions of batteries containing 1,4-BDT additives. Reproduced with permission from Ref.[13] (Copyright 2021, American Chemical Society). (C) Cycling performance of pouch batteries with PhSeH additives. Reproduced with permission from Ref.[48] (Copyright 2022, Springer). (D) Schematic diagram of a Li-S battery with TFP. Reproduced with permission from Ref.[50] (Copyright 2022, American Chemical Society). (E) Schematic diagram of conventional Li-S batteries (left) and batteries containing DPDSe co-mediated (right). Reproduced with permission from Ref.[51] (Copyright 2020, Wiley-VCH GmbH).

Therefore, TFP can effectively inhibit the shuttle effect [Figure 6D]. Zhao *et al.* used diphenyl diselenide (DPDSe) as a redox comediator to accelerate the redox reaction kinetics of sulfur in Li-S batteries [Figure 6E][51]. The DPDSe comediator reduces the energy barrier of the multiphase and multielectron conversion of the sulfide cathode, guarantees fast diffusion kinetics, and changes the deposition dimension of lithium sulfide without causing lithium metal to be damaged during cycling.

## ORGANOSULFIDE CATHODE

Similar to inorganic sulfur, organosulfides can also serve as cathode materials based on the reversible breakage and reformation of S-S bonds during the discharge and charge of the battery[7,52]. The overall charge/discharge processes of linear organosulfides can be described in Equation (2). R is an organic functional group. Organosulfide is a substance with an adjustable structure, unique redox mechanism, and other favorable attributes. By controlling the functional groups, the electrochemical performance of the battery can be adjusted. For example, the introduction of N-containing functional groups can improve the cycle stability of the battery, while the electron-withdrawing functional group can increase the discharge

voltage[52]. At the same time, the battery capacity can be increased by increasing the length of sulfur chains. Although organosulfides have several advantages, their development was not straightforward. As early as the 1980s, organic disulfide was investigated as a cathode material for batteries. However, due to its poor capacity retention and cycle stability, it did not attract much attention[53]. In recent years, with the commercialization of Li-ion batteries and the pursuit of high-energy density batteries, organosulfide batteries have been re-studied and significant advancements have been made. In addition, intriguing redox mechanisms have been revealed. For example, Chen *et al.* reported a small molecule sulfide as a cathode material, i.e., thiuram monosulfide. It does not have electrochemical activity in the voltage range of 2.0-3.0 V. After an initial charge to a high voltage of 3.5 V, it turns out to be a highly reversible cathode material that shows ultra-long and high-rate performance in lithium batteries[54].

$$R\text{-}S_n\text{-}R + (2n-2)\,e^- + (2n-2)\,Li^+ \longleftrightarrow 2R\text{-}SLi + (n-2)\,Li_2S \qquad (2)$$

With the rapid development of organosulfides, some of their drawbacks have gradually emerged. Organosulfide molecules as cathode materials are currently hampered by the fact that they have poor conductivity and the charged and discharged products are easily soluble in the liquid electrolyte[55]. Similar to the sulfur cathode, the shuttle effect also results in the loss of active materials and poor cycle stability. Therefore, to overcome the above challenges, this section summarizes three effective coping strategies: (1) transition metal compounds as the host materials; (2) organic polysulfide polymers as cathode materials; and (3) the use of solid-state electrolytes (SSEs).

**Transition metal compounds**
As host materials, transition metal complexes with excellent electrical conductivity and catalytic activity have been explored. For example, Fan *et al.* used $TiS_2$ nanosheets/CNTs ($TiS_2$ NSs@NWCNT) as the host material for phenyl tetrasulfide (PTS)[56]. Due to the high conductivity and catalytic activity of $TiS_2$, $TiS_2$ NSs@NWCNT can be utilized as a bifunctional mediator that can anchor the discharged product PhSLi and intermediate polysulfides by chemical interactions [Figure 7A], reduce the shuttle effect, and accelerate reaction kinetics. Lv *et al.* grew 1T phase $MoS_2$ *in situ* on the surface of rGO and woven it with CNTs (1T $MoS_2$@rGO/CNTs) as the host material for PTS, as depicted in Figure 7B[57]. 1T $MoS_2$@rGO/CNTs has abundant active sites, which can adsorb soluble PTS and discharge products. During the charging and discharging, the $MoS_2$ dynamic 1T-2H mixed phase can boost electron transport and enhance reaction kinetics. Wang *et al.* utilized diphenyl disulfide (DPDS) as a receptor for sulfur on the cathode of vanadium tetrasulfide on CNTs ($VS_4$/CNTs)[58]. When $VS_4$ as the cathode material is charged to 3 V, $TFSI^-$ in the electrolyte can be intercalated into $VS_4$ [Figure 7C], resulting in the evolution of elemental sulfur. The charge mechanism is as follows: $VS_4 + y\,TFSI^- \rightarrow VS_{(4-y)}\,(TFSI)_y + yS + ye^-$. The battery capacity is reduced by 50% after 50 cycles due to the loss of sulfur. In order to prevent the formation of LiPSs, DPDS is introduced as a sulfur receptor. DPDS and sulfur are chemically combined to generate diphenyl trisulfide (DMTS) during the charge. Figure 7D demonstrates that with the addition of DPDS, the electrochemical performance of the battery has been greatly enhanced. The simplest organic trisulfide, DMTS, has a high theoretical specific capacity of 849 mAh $g^{-1}$. However, DMTS and its charge-discharge products are easily soluble in electrolytes, resulting in a rapid decay in battery capacity. Consequently, He *et al.* developed and synthesized a three-dimensional $Fe_3O_4$/N-graphene sponge (3DFNG) as the host material for DMTS [Figure 7E][15], which could chemically anchor DMTS and its cycled products. A lithium cell with 3DFNG as the host material can be stably cycled for 500 cycles at 1 C.
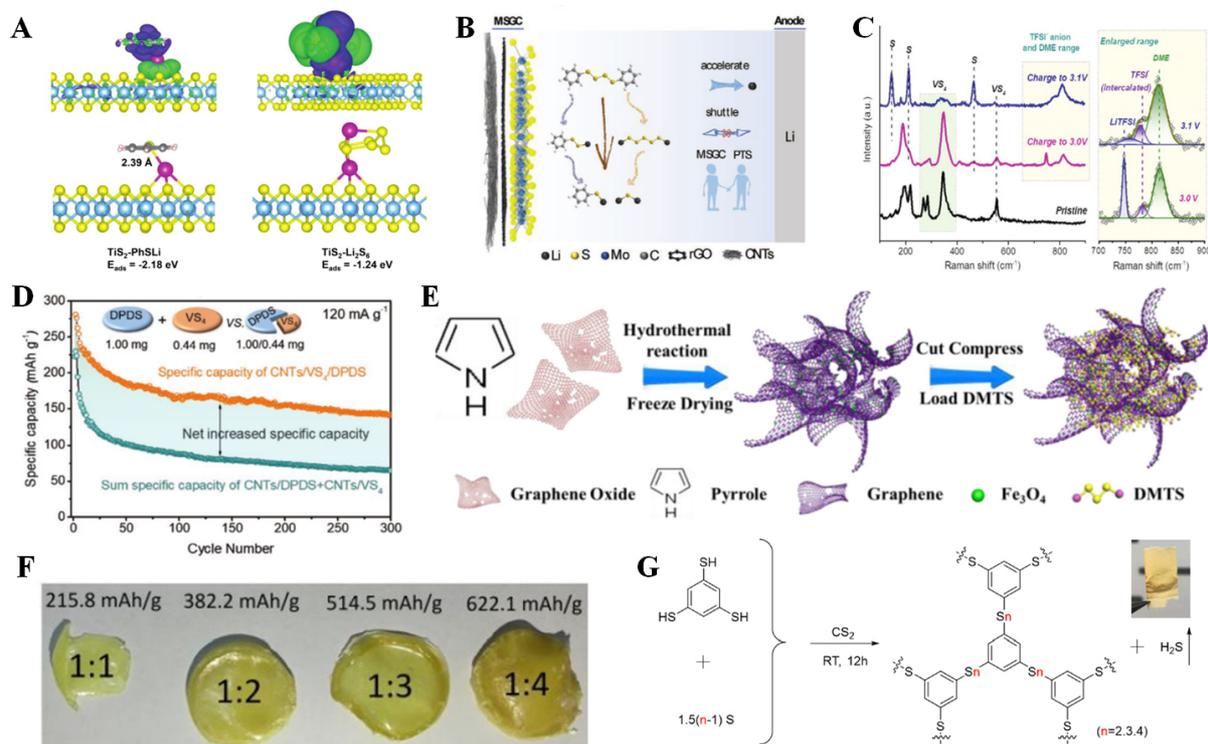
**Figure 7.** (A) PhSLi (left) and $Li_2S_6$ (right) on $TiS_2$ with differential charge contour surfaces in three dimensions. Carbon, hydrogen, lithium, sulfur, and titanium are depicted in gray, white, purple, yellow, and blue. The electronic attachment and detachment densities are represented by surfaces colored blue and green, respectively. Reproduced with permission from Ref.[56] (Copyright 2020, Wiley-VCH GmbH). (B) Schematic diagram of improving battery performance with MSGC substrates. Reproduced with permission from Ref.[57] (Copyright 2021, Wiley-VCH GmbH). (C) $VS_4$ Raman spectra in different charged states (pristine, 3.0 V live and 3.1 V charged). (D) The specific capacity of $CNTs/VS_4/DPDS$ is compared with the total specific capacity of CNTs/DPDS and CNTs/ $VS_4$. Reproduced with permission from Ref.[58] (Copyright 2021, Wiley-VCH GmbH). (E) Synthesis of 3DFNG composites. Reproduced with permission from Ref.[15] (Copyright 2019, Elsevier). (F) Photographs of polymers and their theoretical specific capacity. Reproduced with permission from Ref.[59] (Copyright 2019, The Royal Society of Chemistry). (G) Schematic of BTTP synthesis with different sulfur contents. The inset photo shows the color change of a lead acetate test strip after exposure to the gas produced in the reaction. Reproduced with permission from Ref.[16] (Copyright 2021, Elsevier).

## Organic polysulfide polymers

In comparison to small molecular organosulfides, the specific capacity of most organic polysulfide polymers can exceed 500 mAh g⁻¹, and the sulfur content can be increased by doping extra S. Therefore, organic polysulfide polymers are expected to become a practical and safe cathode material for high-energy batteries. By reacting S with unsaturated olefins, Pyun's group produced copolymers with very high sulfur contents as the cathode materials for batteries in 2013[60]. These copolymers exhibit high specific capacities and capacity retention rates. Using 4, 4′-thiobisbenzenethiol (TBBT) and sulfur, Sang *et al*. produced a class of elastic organic polysulfide polymers[59]. As illustrated in Figure 7F, the sulfur content and theoretical specific capacity of the organic polysulfide polymer may be controlled by the molar ratio of TBBT to S, where the sulfur content can reach up to 50 wt% and the theoretical specific capacity is 622.1 mAh g⁻¹. As depicted in Figure 7G, Sang *et al*. utilized BTT and S as raw materials to synthesize a class of organic polysulfide polymers without heating or additional catalysts[16]. When the molar ratio of BTT:S is 1:4.5, the sulfur content rises to 72 wt%, and the theoretical specific capacity can reach 901.7 mAh g⁻¹. In a lithium battery, the initial discharge capacity can reach 945.1 mAh g⁻¹ at 0.1 C (the higher specific capacity than the theoretical capacity is due to the contribution of CNTs in the electrode). In addition to aromatic polysulfide compounds, aliphatic polysulfide compounds have also been extensively studied. Bhargav *et al*. prepared

polyethylene hexasulfide (PEHS) cathode materials with sulfur content of up to 87 wt% by condensation reaction of 1,2-ethanedithiol with elemental sulfur[61]. The lithium battery using PEHS cathode retains 71% of its initial capacity after 350 cycles at 1 C. Zhou *et al.* used diallyl sulfide and sulfur to prepare an organosulfide cathode with adjustable sulfur atoms in the confined structure[62]. Among them, the prepared poly(diallyl tetrasulfide) cathode exhibits a high capacity of 700 mAh $g^{-1}$ and capacity retention of 85% after 300 cycles. Recently, Zhang *et al.* synthesized disulfide polymers and trisulfide polymers via a sulfur-chain controlling strategy[63]. The experimental and theoretical results show that the sulfur-rich polymers exhibit solid-solid conversion in ether-based electrolytes, thus avoiding the formation of soluble LiPSs and achieving high energy efficiency.

## Solid state electrolytes

The traditional liquid electrolyte is volatile, flammable, and prone to leak, which poses a significant threat to the safety of the battery[64]. Additionally, it is not favorable with the use of organosulfide cathode and lithium metal anode. SSEs are a class of solid ion conductors. The dissolution of the active material is completely suppressed by using SSEs instead of liquid electrolytes. In addition, the application of SSE can prevent battery explosions caused by liquid electrolytes and lithium dendrites piercing the separator, thus enhancing battery safety[65].

Wang *et al.* used $Li_{6.4}La_3Zr_{1.4}Ta_{0.6}O_{12}$ (LLZTO) to replace commercial Celgard as a separator and assembled a semi-solid lithium metal battery with lithium 1,2-benzenedithiolate (LBDT) in liquid electrolyte as the catholyte[66]. Compared to the cell with a Celgard separator, the cell using LLZTO has a capacity retention rate of 65.6% after 100 cycles [Figure 8A]. This suggests that LLZTO can effectively prevent the dissolution of soluble organosulfides during cycling, thereby improving the cycling stability of the battery. Yang *et al.* used poly(trithiocyanuric acid) (PTTCA) as the cathode to assemble all-solid-state Li batteries (ASSLBs) with $Li_7P_3S_{11}$ (LPS) electrolyte [Figure 8B][17]. The experimental results show that SSEs can successfully address the issue of organosulfide dissolution in liquid electrolytes. At room temperature, the PTTCA cathode shows a reversible capacity of 410 mAh $g^{-1}$ under a current rate of 50 mA $g^{-1}$, which is very close to the theoretical specific capacity (450 mAh $g^{-1}$). After 100 cycles, the capacity retention is ~83%. In addition to the above organodisulfides, Ji *et al.* used dipentamethylenethiuram hexasulfide (PMTH) as a cathode material for sulfide-based ASSLBs[67]. The cyclic voltammetry curve of ASSLBs only displays a pair of redox peaks in comparison to batteries using liquid electrolytes, indicating that there is a one-step transition reaction between the charged state (PMTH) and the discharged state ($Li_2S + C_6S_2H_{10}Li$) [Figure 8C]. This indicates that the ASSLBs do not produce soluble LiPSs during cycling, effectively solving the polysulfide shuttle problem.

One of the advantages of organic materials is that we can improve battery performance by adjusting the functional groups of organic molecules. Wang *et al.* found that the oxygen atom of LLZTO can interact with the discharge product (LiSPhSLi), which lowers the charge transfer resistance [Figure 8D][66]. Yang *et al.* found that the N atom on the triazine ring of PTTCA has a lone pair of electrons that can form a coordination bond with $Li^+$ in the LPS electrolyte, allowing for close molecular interaction [Figure 8B][17]. Song *et al.* report a new class of deep eutectic electrolytes (DEEs) induced by Li···N interactions between 2,2′-dipyridyl disulfide (DpyDS) and LiTFSI[68]. The new DEEs exhibit a nonflammable nature and good ionic conductivity. In addition, DEEs are highly viscous and can act as binders. Wang *et al.* adopted the above-reported DEEs as the cathode binder for $LiFePO_4$ (LFP) ASSLBs [Figure 8E], which can well combine conductive carbon and LFP to form intimate contacts between the LLZTO electrolyte and the active material[69].
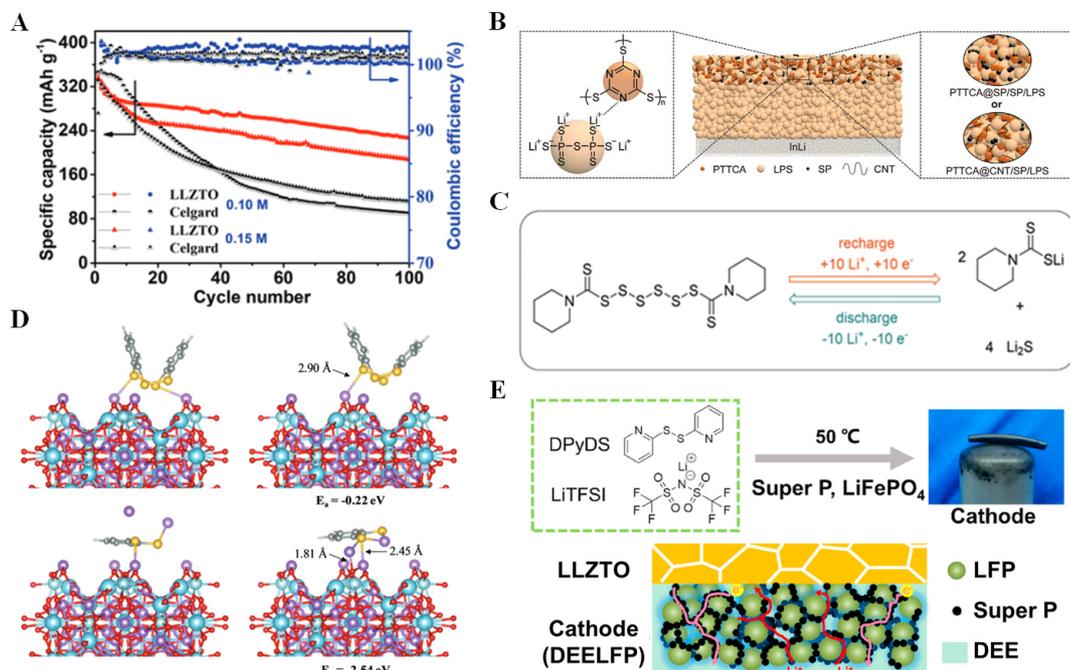
**Figure 8.** (A) Li/LBDT battery cycling performance with Celgard separators or LLZTO. Reproduced with permission from Ref.[66] (Copyright 2022, The Royal Society of Chemistry). (B) Schematic depictions of the ASSLB based on LPS electrolyte and PTTCA cathode (middle), LPS and PTTCA interaction in the cathode (left), and detailed architectures of cathodes employing PTTCA@SP and PTTCA@CNT composites (right). Reproduced with permission from Ref.[17] (Copyright 2021, Wiley-VCH GmbH). (C) Schematic diagram of PMTH molecule charging and discharging. Reproduced with permission from Ref.[67] (Copyright 2022, Wiley-VCH GmbH). (D) On the surface of LLZTO, the initial and optimized structures of the charged product ($Ph_2S_4$) and discharged product (LiSPhSLi) are presented. Lithium, oxygen, carbon, hydrogen, sulfur, and Zirconium (or Tantalum) are depicted in purple, red, gray, white, yellow, and cyan. All of these are with bond distances in Angstroms. Reproduced with permission from Ref.[66] (Copyright 2022, The Royal Society of Chemistry). (E) Schematic diagram of the preparation of DEELFP. Reproduced with permission from Ref.[69] (Copyright 2022, Elsevier).

## OXYGEN CATHODE

A lithium-oxygen batteries (LOBs) consists of a lithium metal anode and oxygen as the cathode[70]. LOBs has an ultra-high energy density (3,500 Wh $kg^{-1}$) and the advantages of environmental friendliness and an abundant oxygen source[71]. During the discharge, the Li on the anode loses an electron to form $Li^+$, and $O_2$ in the cathode is reduced to peroxy-anions ($O_2^{2-}$) by the electrons coming from the anode through the external circuit. $O_2^{2-}$ is subsequently coupled with $Li^+$ to form $Li_2O_2$. The charge is a reversible process. The overall charge/discharge processes of $O_2$ can be described in Equation (3). At present, the electrolyte commonly used in LOBs is an organic liquid, but the generated $Li_2O_2$ is difficult to dissolve in the electrolyte. As a result, the discharge product is deposited at the cathode to block the pores and prevent contact between the electrolyte and oxygen, resulting in poor electrochemical reversibility[72]. At the same time, the slow formation and decomposition kinetics of the insulating discharge products result in large overpotentials. In addition, there are undesirable side reactions on the electrodes of LOBs, which significantly degrade the performance of the batteries[73,74]. The key to resolving the aforementioned issues is the development of highly active cathode catalysts. This section reviews the development of carbon materials, MOFs, metals, and metal oxides as cathode catalysts for LOBs. Table 2 lists the electrochemical properties of different cathode catalysts in Li-$O_2$ batteries.

$$O_2 + 2e^- + 2Li^+ \longleftrightarrow Li_2O_2 \qquad (3)$$

**Table 2. Electrochemical properties of different cathode catalysts in Li-O$_2$ batteries**

| Cathode catalysts | Discharge capacity | Cycles | Ref. |
| --- | --- | --- | --- |
| P-doped (SPC-2) | 20,287.5 mAh g$^{-1}$ at a current density of 200 mA g$^{-1}$ | 226 cycles | [75] |
| Se-doped | 3,942 mAh g$^{-1}$ at a current density of 100 mA g$^{-1}$ | | [76] |
| F-doped (100FC) | 18,230 mAh g$^{-1}$ at a current density of 150 mA g$^{-1}$ | 187 cycles | [18] |
| Ni$^{III}$-NCF | 16,800 mAh g$^{-1}$ at a current density of 500 mA g$^{-1}$ | 200 cycles | [77] |
| NiRu-HTP | 15,080 mAh g$^{-1}$ at a current density of 500 mA g$^{-1}$ | 200 cycles | [78] |
| Tz-Mg-MOF-74 | 7,700 mAh g$^{-1}$ at a current density of 50 mA g$^{-1}$ | | [79] |
| Co-MOF/MXene | 34,763 mAh g$^{-1}$ at a current density of 1,000 mA g$^{-1}$ | 278 cycles | [19] |
| Pt-Pd-Au-Ru | 9,130 mAh g$^{-1}$ at a current density of 100 mA g$^{-1}$ | 20 cycles at a current density of 500 mA g$^{-1}$ | [80] |
| Co/Fe@NC | 17,326 mAh g$^{-1}$ at a current density of 125 mA g$^{-1}$ | 250 cycles | [81] |
| CoFeCe | 12,340 mAh g$^{-1}$ at a current density of 100 mA g$^{-1}$ | over 2,900 h | [20] |
| NiCoFeO@NF | 16,727 mAh g$^{-1}$ at a current density of 500 mA g$^{-1}$ | over 790 h | [82] |

**Carbon material**

Carbon materials have inherent advantages such as excellent electrical conductivity, and adjustable electronic and porous structure. However, traditional carbon materials such as Super P, CNTs, and graphene have limited catalytic activity[83]. With this in mind, various physical and chemical modifications, such as heteroatom doping, have been applied to improve the catalytic activity of carbon materials. The charge redistribution caused by the difference in electronegativity between heteroatoms and carbon atoms can impart carbon with a whole new electrochemical property[84]. Yi *et al*. found through calculations using periodic density functional theory that doping N atoms on the surface of CNTs affects both the atomic distribution and electrical conductivity. N-doped CNT cathode shows increased activity for the adsorption of Li$_x$O$_y$ species compared to CNT cathode[85]. Huang *et al*. synthesized a carbon catalyst obtained from tree sawdust and subjected it to surface phosphatization[75]. The doped P element forms graphitic N-P sites with the nitrogen in pyrrolic-N rather than graphitic C-P sites, which is favorable for preventing the corrosion of tree sawdust carbon during battery cycling. According to theoretical calculations and experimental research, the graphitic N-P sites can be employed as a reaction kinetic promoter for the formation and decomposition of Li$_2$O$_2$. In addition, the P-N sites prevent the corrosion of the carbon catalyst to form the by-product Li$_2$CO$_3$. As a result, the LOBs employing the sawdust-derived P-doped catalysts exhibit outstanding electrochemical performance [Figure 9A]. A typical S-group element with strong oxidation resistance is selenium (Se). A carbon cathode material with selenium was reported by Qian *et al*.[76]. The cathode material has remarkable oxidation resistance, which effectively prevents cathode passivation and side reactions.

In addition to carbon compounds doped with heteroatoms such as N and P, there are rarely reported carbon materials doped with F[84]. Due to the high electronegativity of F, the semi-ionic C-F bond produced by F renders the carbon doped with F acidic and appears as an electron acceptor, leading to an extremely stable material with enhanced electron transfer capability[86,87]. Recently, Ma *et al*. prepared N, O, S, and F co-doped porous carbon materials[18]. The results indicate that appropriate F doping can optimize the electronic structure of the porous carbon substrate so that the affinity between the discharge product Li$_2$O$_2$ and the substrate is moderate. It promotes the adsorption of the product on the surface and the oxygen reduction reaction (ORR) reaction kinetics of the battery. Theoretical calculations reveal that the doped F atoms could easily anchor Li$_2$O$_2$ via the Coulombic force, and it is easy to transport electrons to the electrode via the Li-F-C channel, which facilitates the de-lithiation process of Li$_2$O$_2$. Based on the above characteristics, an appropriate amount of the F-doped porous carbon material applied to the LOBs enables excellent electrochemical performance [Figure 9B].
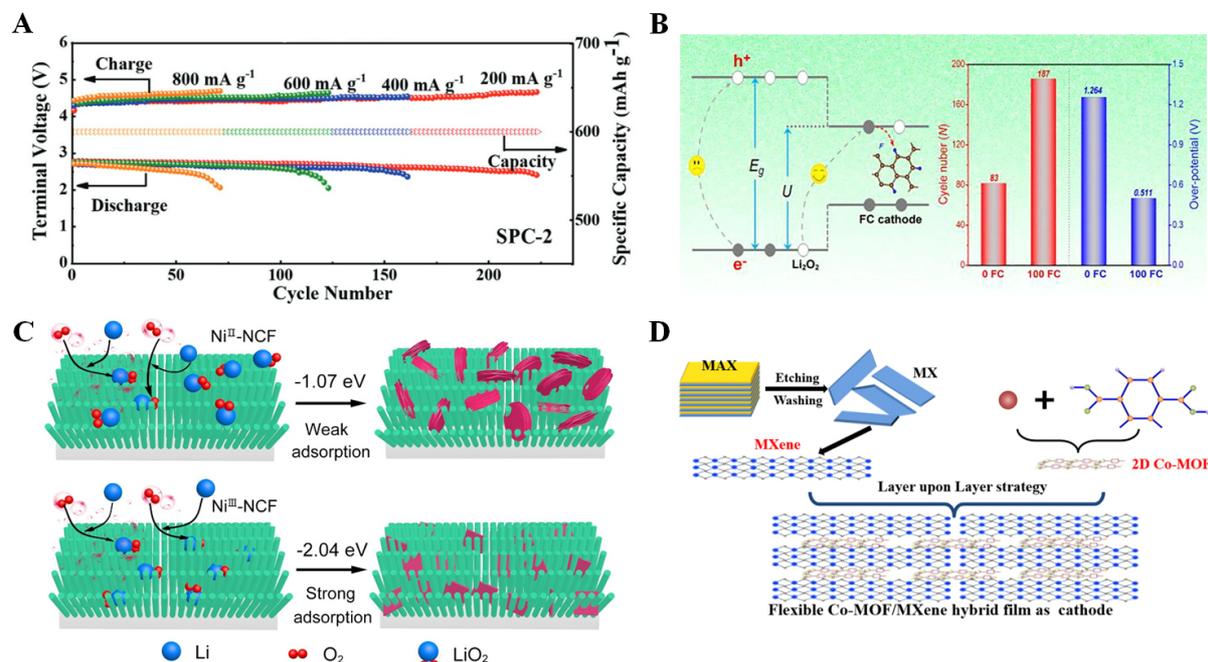
**Figure 9.** (A) Cycling performance at various current densities. Reproduced with permission from Ref.[75] (Copyright 2022, Wiley-VCH GmbH). (B) The corresponding energy barrier reducing mechanism, $E_g$ is the intrinsic excitation energy of $Li_2O_2$, $eU$ is the interfacial charge transfer (ICT) barrier; electrochemical performances of the Li-$O_2$ battery with 0 FC or 100 FC cathode. (Different amounts (0, 100 mg, 200 mg) of tetrafluoroterephthalic acid were used to adjust the content of doped F, and the corresponding products were denoted as 0 FC, 100 FC, and 200 FC, respectively.) Reproduced with permission from Ref.[18] (Copyright 2022, Elsevier). (C) $Ni^{III}$-NCF and $Ni^{II}$-NCF cathode discharge mechanisms. Reproduced with permission from Ref.[77] (Copyright 2021, Wiley-VCH GmbH). (D) preparation of the flexible hybrid free-standing film using a layer-by-layer approach. Reproduced with permission from Ref.[19] (Copyright 2021, Elsevier).

## Metal-organic frameworks

Metal-organic frameworks (MOFs) are a class of porous materials with adjustable composition and controllable pore size structure. MOFs and their derivatives can be employed as catalysts for LOBs due to their atomically dispersed metal centers and large specific surface area[88]. The electrocatalytic activity of a catalyst is closely related to the electronic structure of its central metal, such as its spin configuration and oxidation state, which affects its performance[89]. Lv *et al.* obtained a conductive nickel catecholate framework ($Ni^{III}$-NCF) as a bifunctional catalyst by adjusting the spin state of the $Ni^{2+}$ site of $Ni^{II}$-NCF. The regulation of the spin state enhances the covalence of nickel-oxygen in $Ni^{III}$-NCF[77], promotes the electron exchange between the Ni site and the oxygen adsorbent, and accelerates the redox kinetics of oxygen. The high affinity of the $Ni^{3+}$ site with the intermediate $LiO_2$ promotes the formation of $Li_2O_2$ nanosheets in the void space of $Ni^{III}$-NCF nanowires after discharge [Figure 9C]. This reduces the battery overpotential and improves rate performance and cycle stability. Recently, Lv *et al.* designed the conductive bimetallic MOF NiRu-hexaiminotriphenylene (NiRu-HTP) by ion exchange and employed it as a useful cathode catalyst for LOBs. NiRu-HTP has a higher current density, a higher ORR initial potential of 2.76 V, and a lower OER starting potential of 2.98 V than Ni-hexaiminotriphenylene (Ni-HTP). Additionally, the NiRu-HTP-based LOBs exhibit a 0.76 V lower charge/discharge polarization[78]. Currently, the majority of related research focuses on adding redox-active metal centers to MOFs. Furthermore, organic redox-active compounds may be added to MOFs. To create a 1,2,4,5-tetrazine (Tz)-Mg-MOF-74 cathode for LOBs, Li *et al.* anchored redox-active Tz molecules in porous MOFs[79]. The benefits of MOF structure and organic redox molecules can be used to improve the electrochemical performance of MOF-based electrode materials by accelerating the electrochemical reaction kinetics of LOBs during charge and discharge.
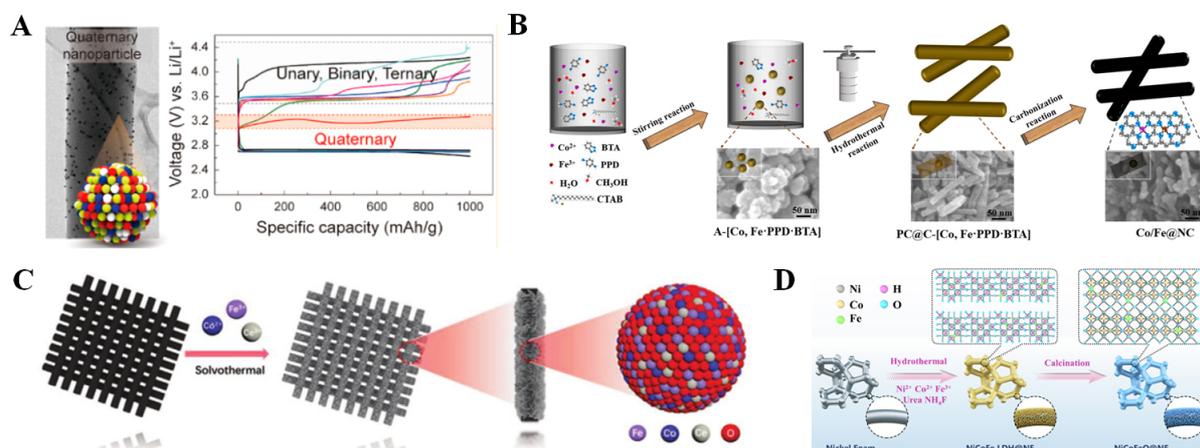
**Figure 10.** (A) Schematic diagram of quaternary nanoparticles and their voltage comparison. Reproduced with permission from Ref.[80] (Copyright 2021, American Chemical Society). (B) Synthetic method for the production of Co/Fe@NC and scanning electron microscope images of A-[Co, Fe·PPD·BTA], PC@C-[Co, Fe·PPD·BTA], and Co/Fe@NC. Reproduced with permission from Ref.[81] (Copyright 2022, American Chemical Society). (C) Illustration of the manufacturing of CoFeCe-2. Reproduced with permission from Ref.[20] (Copyright 2021, Wiley-VCH GmbH). (D) Preparation of arrays of NiCoFeO@NF nanowires. Reproduced with permission from Ref.[82] (Copyright 2021, Elsevier).

The traditional slurry preparation process of cathodes could result in catalyst agglomeration and poor uniformity. Zhang *et al.* inserted 2D Co-MOF nanosheets between MXene layers based on a layer-upon-layer self-assembly strategy to prepare a self-supporting flexible Co-MOF/MXene hybrid film [Figure 9D][19]. It has a two-dimensional sheet structure and high ORR catalytic activity, which can provide fast $Li^+/O_2$ transport channels and promote the formation and decomposition of $Li_2O_2$. LOBs based on Co-MOF/MXene composite film as the cathode exhibit ultra-high capacity (34,763 mAh $g^{-1}$ at a current density of 1,000 mA $g^{-1}$) and excellent cycle stability (278 cycles, limited capacity of 1,000 mAh $g^{-1}$ at a current density of 1,000 mA $g^{-1}$).

**Metals and metal oxides**
Metals and metal oxides are regarded as ideal catalysts for LOBs due to their excellent catalytic effect on the formation and decomposition of $Li_2O_2$, which can significantly lower the overpotential of the battery and improve cycle stability[90]. The employment of precious metal catalysts in LOBs improves $O_2$ binding energy, which is favorable to the second electron transfer, hence boosting the formation of $Li_2O_2$. Simultaneously, it can decrease the decomposition energy barrier of $Li_2O_2$ and achieve fast diffusion of $O_2$. Polymetallic catalysts can exert synergistic catalytic effects and improve the electrochemical performance of LOBs compared to single-metal catalysts. Jung *et al.* prepared 14 oxygen cathode catalysts composed of four elements: Pt, Pd, Au, and Ru, on carbon nanofibers by the joule heating route[80]. As shown in Figure 10A, the quaternary nanoparticles (Pt-Pd-Au-Ru) exhibit the lowest overpotential (~0.45 V) and highest discharge capacity (9,130 mAh $g^{-1}$, based on total cathode mass).

Due to the high price and scarcity of resources, the widespread use of precious metals is limited, while other transition metals with relatively inexpensive costs and good catalytic activity have been studied. Li *et al.* developed an organic bimetallic coordination polymer based on Co and Fe [Figure 10B] in the form of rod-like N-doped carbon (Co/Fe@NC) coated with Co and Fe nanoparticles that were employed as a cathode catalyst for LOBs[81]. The rod of N-doped carbon not only improves conductivity but also provides rich pores for the diffusion of $Li^+$ and $O_2$. Doped bimetals can greatly enhance ORR/OER activity; $Fe-N_x$ sites are advantageous for enhancing ORR activity, and so are the dosed $Co-N_x$ sites. The use of Co/Fe@NC as a

cathode catalyst enables the battery to cycle stably for more than 250 cycles and to display a high discharge capacity of 17,326 mAh g$^{-1}$. Transition metal oxides can also catalyze the formation and decomposition of $Li_2O_2$. Sun *et al*. prepared ternary metal oxides $(CoFeCeO_x)$ with amorphous/crystalline heterostructures by a one-step solvothermal method and prepared highly active $CoFeCeO_x$ cathode catalysts with kinetic and thermodynamic stability by precisely adjusting the ratios of Co, Fe, and Ce [Figure 10C][20]. Due to the coexistence of amorphous and crystalline domains, abundant active sites are exposed, the adsorption of the intermediate product $LiO_2$ is enhanced, and the ORR reaction kinetics is improved. As shown in Figure 10D, Ren *et al*. synthesized Fe-doped binary $NiCo_2O_4$ (NiCoFeO@NF) as a cathode catalyst. Based on theoretical calculations[82], the introduction of iron in $NiCo_2O_4$ can adjust the transition metal-3d-$e_g$ electron occupancy, thereby increasing the covalent of the transition metal-oxygen bond, reducing the energy barrier of $Li_2O_2$ formation and decomposition, making the discharge capacity of the battery as high as 16,727 mAh g$^{-1}$.

## CONCLUSION AND OUTLOOK

Conversion-based electrode materials have the advantages of high theoretical specific capacity and energy density, which can meet the increasing demand for large-scale energy storage. In recent years, lithium-sulfur and lithium-organosulfide batteries have been developed rapidly and are expected to be close to commercial applications. Lithium-oxygen batteries use oxygen as the active material, which has the advantages of ultra-high energy density and sustainability. This review summarizes the recent research efforts on the above three conversion-based electrode materials, including the use of a variety of cathode host materials, electrolyte additives, solid-state electrolytes, cathode catalysts, and other strategies to improve the electrochemical performance of batteries, aiming to realize a new generation of safe and efficient energy storage systems.

Although conversion-based electrode materials have great advantages, they still face challenges for practical applications, such as poor conductivity, high solubility, high dependence on electrolyte, *etc*. Therefore, future research efforts should be focused on the following aspects: (1) development of novel, highly conductive carbon-based or nitrogen-doped electrode materials to increase the utilization of active materials; (2) development of electrolytes to decrease the solubility of active materials; (3) application of solid-state electrolytes to reduce the crossover of active materials and improve battery safety; (4) exploration of conversion-based electrode materials in a variety of battery systems, such as Na, Mg, liquid flow, *etc*.; (5) introduction of advanced characterization techniques to reveal redox mechanisms of batteries; and (6) development of low-cost, simple synthesis methods to meet large-scale production. In summary, conversion-based electrode materials have the potential to meet future energy storage needs, and we hope that this review can inspire more interest in developing new electrode materials that can enable high-energy battery systems for future applications.

## DECLARATIONS

**Authors' contributions**
Proposed the topic of this review: Fu Yz
Prepared the manuscript: Ren Y, Fan Js
Collectively discussed and revised the manuscript: Ren Y, Fan Js, Fu Yz

**Availability of data and materials**
Not applicable.

**Conflicts of interest**

All authors declared that there are no conflicts of interest.

**Ethical approval and consent to participate**

Not applicable.

**Consent for publication**

Not applicable.

## REFERENCES

1. Deng D. Li-ion batteries: basics, progress, and challenges. *Energy Sci Eng* 2015;3:385-418. DOI
2. Pender JP, Jha G, Youn DH, et al. Electrode degradation in lithium-ion batteries. *ACS Nano* 2020;14:1243-95. DOI
3. Mukhopadhyay A, Sheldon BW. Deformation and stress in electrode materials for Li-ion batteries. *Prog Mater Sci* 2014;63:58-116. DOI
4. Manthiram A. A reflection on lithium-ion battery cathode chemistry. *Nat Commun* 2020;11:1550. DOI PubMed PMC
5. Yin YX, Xin S, Guo YG, Wan LJ. Lithium-sulfur batteries: electrochemistry, materials, and prospects. *Angew Chem Int Ed* 2013;52:13186-200. DOI PubMed
6. Zhao M, Li BQ, Zhang XQ, Huang JQ, Zhang Q. A perspective toward practical lithium-sulfur batteries. *ACS Cent Sci* 2020;6:1095-104. DOI PubMed PMC
7. Guo W, Wang DY, Chen Q, Fu Y. Advances of organosulfur materials for rechargeable metal batteries. *Adv Sci* 2022;9:e2103989. DOI PubMed PMC
8. Feng N, He P, Zhou H. Critical challenges in rechargeable aprotic Li-O$_2$ batteries. *Adv Energy Mater* 2016;6:1502303. DOI
9. Shu C, Wang J, Long J, Liu HK, Dou SX. Understanding the reaction chemistry during charging in aprotic lithium-oxygen batteries: existing problems and solutions. *Adv Mater* 2019;31:e1804587. DOI PubMed
10. Chen Y, Wang T, Tian H, Su D, Zhang Q, Wang G. Advances in lithium-sulfur batteries: from academic research to commercial viability. *Adv Mater* 2021;33:e2003666. DOI PubMed
11. Hong X, Liu Y, Fu J, et al. A wheat flour derived hierarchical porous carbon/graphitic carbon nitride composite for high-performance lithium-sulfur batteries. *Carbon* 2020;170:119-26. DOI
12. Li Y, Zeng Y, Chen Y, Luan D, Gao S, Lou XWD. Mesoporous N-rich carbon with single-Ni atoms as a multifunctional sulfur host for Li-S batteries. *Angew Chem Int Ed* 2022;61:e202212680. DOI PubMed
13. Lian J, Guo W, Fu Y. Isomeric organodithiol additives for improving interfacial chemistry in rechargeable Li-S batteries. *J Am Chem Soc* 2021;143:11063-71. DOI PubMed
14. Guo W, Zhang W, Si Y, Wang D, Fu Y, Manthiram A. Artificial dual solid-electrolyte interfaces based on in situ organothiol transformation in lithium sulfur battery. *Nat Commun* 2021;12:3031. DOI PubMed PMC
15. He J, Bhargav A, Manthiram A. Three-dimensional Fe$_3$O$_4$/N-graphene sponge as an efficient organosulfide host for high-performance lithium-organosulfur batteries. *Energy Stor Mater* 2019;23:88-94. DOI
16. Sang P, Song J, Guo W, Fu Y. Hyperbranched organosulfur polymer cathode materials for Li-S battery. *Chem Eng J* 2021;415:129043. DOI
17. Yang Z, Wang F, Hu Z, et al. Room-temperature all-solid-state lithium-organic batteries based on sulfide electrolytes and organodisulfide cathodes. *Adv Energy Mater* 2021;11:2102962. DOI
18. Ma S, Yao H, Li Z, Liu Q. Tuning the nucleation and decomposition of Li$_2$O$_2$ by fluorine-doped carbon vesicles towards high performance Li-O$_2$ batteries. *J Energy Chem* 2022;70:614-22. DOI
19. Zhang W, Tang S, Chen Z, et al. The controllable construction of nanochannel in two-dimensional lamellar film for efficient oxygen reduction reaction and lithium-oxygen batteries. *Chem Eng J* 2022;430:132489. DOI
20. Sun Z, Cao X, Tian M, et al. Synergized multimetal oxides with amorphous/crystalline heterostructure as efficient electrocatalysts for lithium-oxygen batteries. *Adv Energy Mater* 2021;11:2100110. DOI
21. Ji X, Evers S, Lee KT, Nazar LF. Agitation induced loading of sulfur into carbon CMK-3 nanotubes: efficient scavenging of noble metals from aqueous solution. *Chem Commun* 2010;46:1658-60. DOI PubMed
22. Chung SH, Manthiram A. Current status and future prospects of metal-sulfur batteries. *Adv Mater* 2019;31:e1901125. DOI PubMed

23. Seh ZW, Sun Y, Zhang Q, Cui Y. Designing high-energy lithium-sulfur batteries. *Chem Soc Rev* 2016;45:5605-34. DOI PubMed
24. Zhang L, Wang Y, Niu Z, Chen J. Advanced nanostructured carbon-based materials for rechargeable lithium-sulfur batteries. *Carbon* 2019;141:400-16. DOI
25. Hu Q, Dong H, Wang B, et al. Constructing coral-like hierarchical porous carbon architectures with tailored pore size distribution as sulfur hosts for durable Li-S batteries. *Electrochim Acta* 2021;377:138063. DOI
26. Zhang Y, Li G, Wang J, et al. "Sauna" activation toward intrinsic lattice deficiency in carbon nanotube microspheres for high-energy and long-lasting lithium-sulfur batteries. *Adv Energy Mater* 2021;11:2100497. DOI
27. Shi K, Lin Y, Li J, Xiong Z, Liao J, Liu Q. Carbon-based cathode host derived from crosslinked porous polyimides for lithium-sulfur batteries and their electrochemical properties. *Int J Hydrog Energy* 2022;47:21662-72. DOI
28. Liu Y, Guo H, Zhang B, et al. Sustainable synthesis of N-doped hollow porous carbon spheres via a spray-drying method for lithium-sulfur storage with ultralong cycle life. *Batteries Supercaps* 2020;3:1201-8. DOI
29. Yang Z, Jia D, Zhao Q, et al. Multichalcogen-integrated cathodes for novel lithium-chalcogenide batteries in ether and ester electrolytes. *ACS Appl Mater Interfaces* 2022;14:32112-23. DOI PubMed
30. Zhou L, Danilov DL, Eichel R, Notten PHL. Host materials anchoring polysulfides in Li-S batteries reviewed. *Adv Energy Mater* 2021;11:2001304. DOI
31. Lin Y, Li J, Xiong Z, Shi K, Liu Q. Carbon-based conductive frameworks and metal catalytic sites derived from cross-linked porous porphyrin-based polyimides for enhanced conversion of lithium polysulfides in Li-S batteries. *ACS Appl Energy Mater* 2021;4:14497-507. DOI
32. Su L, Zhang J, Chen Y, et al. Cobalt-embedded hierarchically-porous hollow carbon microspheres as multifunctional confined reactors for high-loading Li-S batteries. *Nano Energy* 2021;85:105981. DOI
33. Zhang B, Wang L, Wang B, et al. Petroleum coke derived porous carbon/NiCoP with efficient reviving catalytic and adsorptive activity as sulfur host for high performance lithium - sulfur batteries. *Nano Res* 2022;15:4058-67. DOI
34. Li W, Jin X, Xiao L, et al. Enhancing polysulfide confinement and conversion in meso-/microporous core-shelled MoC/NC microspheres for lithium-sulfur batteries. *J Mater Chem A* 2021;9:26051-60. DOI
35. Kang X, Dong Y, Guan H, Al-Tahan MA, Zhang J. Manipulating the electrocatalytic activity of sulfur cathode via distinct cobalt sulfides as sulfur host materials in lithium-sulfur batteries. *J Colloid Interface Sci* 2022;622:515-25. DOI PubMed
36. Wang YP, Li ZS, Cao XR, Wu SQ, Zhu ZZ. Monolayer $MSi_2P_4$ (M = V, Nb, and Ta) as highly efficient sulfur host materials for lithium-sulfur batteries. *ACS Appl Mater Interfaces* 2022;14:27833-41. DOI PubMed
37. Wei Z, Ren Y, Sokolowski J, Zhu X, Wu G. Mechanistic understanding of the role separators playing in advanced lithium-sulfur batteries. *InfoMat* 2020;2:483-508. DOI
38. Wu N, Wang J, Liao C, et al. A flame retardant separator modified by MOFs-derived hybrid for safe and efficient Li-S batteries. *J Energy Chem* 2022;64:372-84. DOI
39. Wang M, Han S, Chao Z, et al. Celgard-supported LiX zeolite membrane as ion-permselective separator in lithium sulfur battery. *J Membr Sci* 2020;611:118386. DOI
40. Wang Y, Zhu L, Wang J, Zhang Z, Yu J, Yang Z. Enhanced chemisorption and catalytic conversion of polysulfides via CoFe@NC nanocubes modified separator for superior Li-S batteries. *Chem Eng J* 2022;433:133792. DOI
41. Yu X, Wu H, Koo JH, Manthiram A. Tailoring the pore size of a polypropylene separator with a polymer having intrinsic nanoporosity for suppressing the polysulfide shuttle in lithium-sulfur batteries. *Adv Energy Mater* 2019;10:1902872. DOI
42. Peng J, Zhu J, Wang Y, Xu M, Jiang J. Thermotolerant and $Li_2Sn$-trapped/converted separators enabled by $NiFe_2O_4$ quantum dots/g-$C_3N_4$ nanofiber interlayers: toward more practical Li-S batteries. *Mater Chem Front* 2022;6:2034-41. DOI
43. Tan L, Li X, Wang Z, Guo H, Wang J. Lightweight reduced graphene Oxide@$MoS_2$ interlayer as polysulfide barrier for high-performance lithium-sulfur batteries. *ACS Appl Mater Interfaces* 2018;10:3707-13. DOI
44. Hu Q, Lu J, Yang C, et al. Promoting reversible redox kinetics by separator architectures based on $CoS_2$/HPGC interlayer as efficient polysulfide-trapping shield for Li-S batteries. *Small* 2020;16:e2002046. DOI PubMed
45. Kim S, Shirvani-Arani S, Choi S, Cho M, Lee Y. Strongly anchoring polysulfides by hierarchical $Fe_3O_4$/$C_3N_4$ nanostructures for advanced lithium-sulfur batteries. *Nanomicro Lett* 2020;12:139. DOI PubMed PMC
46. Lee BJ, Zhao C, Yu JH, et al. Development of high-energy non-aqueous lithium-sulfur batteries via redox-active interlayer strategy. *Nat Commun* 2022;13:4629. DOI PubMed PMC
47. Cao R, Xu W, Lv D, Xiao J, Zhang J. Anodes for rechargeable lithium-sulfur batteries. *Adv Energy Mater* 2015;5:1402273. DOI
48. Sun J, Zhang K, Fu Y, Guo W. Benzoselenol as an organic electrolyte additive in Li-S battery. *Nano Res* 2023;16:3814-22. DOI
49. Wang D, Wang W, Li F, Li X, Guo W, Fu Y. Nitrogen-rich azoles as trifunctional electrolyte additives for high-performance lithium-sulfur battery. *J Energy Chem* 2022;71:572-9. DOI
50. Jiang C, Li L, Jia Q, et al. In situ synthesis of organopolysulfides enabling spatial and kinetic co-mediation of sulfur chemistry. *ACS Nano* 2022;16:9163-71. DOI PubMed
51. Zhao M, Chen X, Li XY, Li BQ, Huang JQ. An organodiselenide comediator to facilitate sulfur redox kinetics in lithium-sulfur batteries. *Adv Mater* 2021;33:e2007298. DOI PubMed
52. Wang DY, Guo W, Fu Y. Organosulfides: an emerging class of cathode materials for rechargeable lithium batteries. *ACC Chem Res* 2019;52:2290-300. DOI PubMed
53. Visco SJ, Dejonghe LC. Ionic conductivity of organosulfur melts for advanced storage electrodes. *J Electrochem Soc* 1988;135:2905-

9.   DOI

54.   Chen Q, Li L, Wang W, Li X, Guo W, Fu Y. Thiuram monosulfide with ultrahigh redox activity triggered by electrochemical oxidation. *J Am Chem Soc* 2022;144:18918-26.  DOI  PubMed

55.   Pan Q, Lan J, Si Y, Guo W, Fu Y. A fluorinated macrocyclic organodisulfide cathode for lithium organic batteries. *Chem Commun* 2022;58:5602-5.  DOI  PubMed

56.   Fan Q, Guo W, Si Y, Wang X, Wang B, Fu Y. Inorganic mediator toward organosulfide active material: anchoring and electrocatalysis. *Adv Funct Mater* 2021;31:2001493.  DOI

57.   Lv X, Guo W, Song J, Fu Y. Dynamic 1T-2H mixed-phase $MoS_2$ enables high-performance Li-organosulfide battery. *Small* 2022;18:e2105071.  DOI  PubMed

58.   Wang Z, Li X, Guo W, Fu Y. Anion intercalation of $VS_4$ triggers atomic sulfur transfer to organic disulfide in rechargeable lithium battery. *Adv Funct Mater* 2021;31:2009875.  DOI

59.   Sang P, Si Y, Fu Y. Polyphenyl polysulfide: a new polymer cathode material for Li-S batteries. *Chem Commun* 2019;55:4857-60. DOI  PubMed

60.   Chung WJ, Griebel JJ, Kim ET, et al. The use of elemental sulfur as an alternative feedstock for polymeric materials. *Nat Chem* 2013;5:518-24.  DOI  PubMed

61.   Bhargav A, Chang CH, Fu Y, Manthiram A. Rationally designed high-sulfur-content polymeric cathode material for lithium-sulfur batteries. *ACS Appl Mater Interfaces* 2019;11:6136-42.  DOI  PubMed

62.   Zhou J, Zhou X, Sun Y, Shen X, Qian T, Yan C. Insight into the reaction mechanism of sulfur chains adjustable polymer cathode for high-loading lithium-organosulfur batteries. *J Energy Chem* 2021;56:238-44.  DOI

63.   Zhang X, Hu G, Chen K, et al. Structure-related electrochemical behavior of sulfur-rich polymer cathode with solid-solid conversion in lithium-sulfur batteries. *Energy Stor Mater* 2022;45:1144-52.  DOI

64.   Kim JG, Son B, Mukherjee S, et al. A review of lithium and non-lithium based solid state batteries. *J Power Sources* 2015;282:299-322.  DOI

65.   Manthiram A, Yu X, Wang S. Lithium battery chemistries enabled by solid-state electrolytes. *Nat Rev Mater* 2017;2:16103.  DOI

66.   Wang B, Jin Y, Si Y, Guo W, Fu Y. Garnet solid-state electrolyte with benzenedithiolate catholyte for rechargeable lithium batteries. *Chem Commun* 2022;58:3657-60.  DOI  PubMed

67.   Ji W, Zhang X, Zheng D, Huang H, Lambert TH, Qu D. Practically accessible all-solid-state batteries enabled by organosulfide cathodes and sulfide electrolytes. *Adv Funct Mater* 2022;32:2202919.  DOI

68.   Song J, Si Y, Guo W, Wang D, Fu Y. Organosulfide-based deep eutectic electrolyte for lithium batteries. *Angew Chem Int Ed* 2021;60:9881-5.  DOI  PubMed

69.   Wang B, Guo W, Fu Y. High-performance garnet solid-state battery enabled by improved interfaces. *J Power Sources* 2022;542:231798.  DOI

70.   Dou Y, Xie Z, Wei Y, Peng Z, Zhou Z. Redox mediators for high-performance lithium-oxygen batteries. *Natl Sci Rev* 2022;9:nwac040.  DOI  PubMed  PMC

71.   Shen X, Liu H, Cheng X, Yan C, Huang J. Beyond lithium ion batteries: higher energy density battery systems based on lithium metal anodes. *Energy Stor Mater* 2018;12:161-75.  DOI

72.   Lu Y, Gallant BM, Kwabi DG, et al. Lithium-oxygen batteries: bridging mechanistic understanding and battery performance. *Energy Environ Sci* 2013;6:750-68.  DOI

73.   Zhang H, Eshetu GG, Judez X, Li C, Rodriguez-Martínez LM, Armand M. Electrolyte additives for lithium metal anodes and rechargeable lithium metal batteries: progress and perspectives. *Angew Chem Int Ed* 2018;57:15002-27.  DOI  PubMed

74.   Chen K, Yang D, Wang J, Huang G, Zhang X. Overcharge to remove cathode passivation layer for reviving failed $Li-O_2$ batteries. *CCS Chem* 2023;5:641-53.  DOI

75.   Huang H, Cheng C, Zhang G, et al. Surface phosphatization for a sawdust-derived carbon catalyst as kinetics promoter and corrosion preventer in lithium-oxygen batteries. *Adv Funct Mater* 2022;32:2111546.  DOI

76.   Qian Z, Guo R, Ma Y, et al. Se-doped carbon as highly stable cathode material for high energy nonaqueous $Li-O_2$ batteries. *Chem Eng Sci* 2020;214:115413.  DOI

77.   Lv Q, Zhu Z, Ni Y, Geng J, Li F. Spin-state manipulation of two-dimensional metal-organic framework with enhanced metal-oxygen covalency for lithium-oxygen batteries. *Angew Chem Int Ed* 2022;61:e202114293.  DOI  PubMed

78.   Lv Q, Zhu Z, Ni Y, et al. Atomic ruthenium-riveted metal-organic framework with tunable d-band modulates oxygen redox for lithium-oxygen batteries. *J Am Chem Soc* 2022;144:23239-46.  DOI  PubMed

79.   Li N, Chang Z, Zhong M, et al. Functionalizing MOF with redox-active tetrazine moiety for improving the performance as cathode of $Li-O_2$ batteries. *CCS Chem* 2021;3:1297-305.  DOI

80.   Jung WB, Park H, Jang JS, et al. Polyelemental nanoparticles as catalysts for a $Li-O_2$ battery. *ACS Nano* 2021;15:4235-44.  DOI

81.   Li D, Liang J, Robertson SJ, et al. Heterogeneous bimetallic organic coordination polymer-derived Co/Fe@NC bifunctional catalysts for rechargeable $Li-O_2$ batteries. *ACS Appl Mater Interfaces* 2022;14:5459-67.  DOI

82.   Ren L, Zheng R, Du D, et al. Optimized orbital occupancy of transition metal in spinel Ni-Co oxides with heteroatom doping for Aprotic $Li-O_2$ battery. *Chem Eng J* 2022;430:132977.  DOI

83.   Hu C, Paul R, Dai Q, Dai L. Carbon-based metal-free electrocatalysts: from oxygen reduction to multifunctional electrocatalysis. *Chem Soc Rev* 2021;50:11785-843.  DOI  PubMed

84.  Zheng X, Wu J, Cao X, et al. N-, P-, and S-doped graphene-like carbon catalysts derived from onium salts with enhanced oxygen chemisorption for Zn-air battery cathodes. *Appl Catal B Environ* 2019;241:442-51.  DOI

85.  Yi X, Liu X, Dou R, Wen Z, Zhou W. Understanding the catalytic activity of the preferred nitrogen configuration on the carbon nanotube surface and its implications for Li-O$_2$ batteries. *J Phys Chem C* 2021;125:22570-80.  DOI

86.  Zhou J, Lian J, Hou L, et al. Ultrahigh volumetric capacitance and cyclic stability of fluorine and nitrogen co-doped carbon microspheres. *Nat Commun* 2015;6:8503.  DOI  PubMed  PMC

87.  Wang T, Zang X, Wang X, Gu X, Shao Q, Cao N. Recent advances in fluorine-doped/fluorinated carbon-based materials for supercapacitors. *Energy Stor Mater* 2020;30:367-84.  DOI

88.  Li Z, Gao R, Feng M, et al. Modulating metal-organic frameworks as advanced oxygen electrocatalysts. *Adv Energy Mater* 2021;11:2003291.  DOI

89.  Shen G, Zhang R, Pan L, et al. Regulating the spin state of Fe$^{III}$ by atomically anchoring on ultrathin titanium dioxide for efficient oxygen evolution electrocatalysis. *Angew Chem Int Ed* 2020;132:2333-7.  DOI  PubMed

90.  Balaish M, Jung J, Kim I, Ein-eli Y. A critical review on functionalization of air-cathodes for nonaqueous Li-O$_2$ batteries. *Adv Funct Mater* 2020;30:1808303.  DOI